Measurements and Modelling of Full-Scale Concentration Fluctuations

Open-field experiments using krypton-85 and tetrahydrothiophen as tracers

Thomas Lung[1)], Hans-Joachim Müller[2)], Manfred Gläser[2)] and **Bernd Möller[2)]**
[1)] Ingenieurbüro Berlin
[2)] Institut für Agrartechnik Bornim, Potsdam-Bornim

The simulation of odour frequencies near animal housing facilities or industrial plants requires a model of the frequency distribution of concentration. Generally, for this purpose two-parameter distribution functions are used, which, depending upon the mean value and the variance of odour concentration, provide information about the probability of occurrence. In order to examine how well the simulations coincide with reality, the calculation results are compared with measurement data. In model construction this examination step is also termed validation.
Open-field experiments with tracers serve to examine the dispersion and fluctuation behaviour of airborne material in the atmospheric wind field. If in particular one intends to analyze the concentration fluctuations of odours, measuring techniques with high temporal resolution must be employed because odours can be perceived by the human nose within one second. In this examination, the artificially produced gas krypton-85 serves as a tracer, whose concentration was measured by a group of detectors each at different distances from the source in one-second intervals. Based on the measurement data, mean values, variance, and higher statistical moments of the tracer concentration are calculated and compared with the corresponding results of model simulations. Observed and simulated exceedance probabilities are compared, and the statistical characteristics of the models used are discussed.
Do the results of the tracer measurement can be directly applied to odour frequencies? In order to answer this question, in some field experiments, the odourant tetrahydrothiophen, whose odour effects were registered by test persons at selected detector positions, was released at the same time as the tracer krypton-85. In contrast to the precise, unambiguous tracer measurement, the perception and assessment of odours is dependent upon sensation so that the application of the exceedance probability determined through measurement to the frequency of sensory perception needs to be statistically validated.

Keywords
Concentration fluctuations, probability density function, impacts of odour, tracer measurement, krypton-85, turbulent dispersion

Introduction

Reliable odour impact predictions are not only needed in permit procedures for plants and facilities. To an increasing extent, they are also required as an instrument for the monitoring of facilities for which permission has already been granted and in cases of civil lawsuit. In any case, however, dispersion simulation is intended to reflect the determined odour perceptions of affected residents as precisely as possible using probability of occurrence and intensity as criteria. Given these considerations, the modelling of fluctuating odour concentrations plays a key role because the standard deviation is usually at least as large as the mean value of concentration. The validation of such "fluctuation models" requires a comparison of simulation results and corresponding measurements. In the past two decades, increasing research activity in the area of fluctuation measurements could be noticed. However, the majority of these measurements were taken in the wind tunnel or the water channel, whereas there are few publications about full-scale fluctuation experiments with suitable tracers based on examination methods that are not very systematic. To the authors' knowledge, open-field fluctuation measurements with high temporal resolution in connection with olfactory immission measurements of a simultaneously released odourant have not been reported on thus far.
For the simulation of exceedance frequencies of given odour threshold values, statistical approaches are preferably employed. For these statistical or stochastic approaches, the choice of a suitable density function is of crucial importance. This function must reflect the frequency distribution of the observed odour concentrations with sufficient precision. In the present paper, we will confine ourselves to the examination of some of the two-parameter density functions which are sufficiently flexible with regard to data adaptation and at the same time easy to use in model construction. One of the two parameters is functionally connected with the *mean value* of the concentration, while the other parameter is a measure of the *variance* of the concentration, i.e. of the intensity of the fluctuations. All density functions which are employed to describe the exceedance frequencies of given threshold values have a pronounced empirical character. They cannot easily be founded theoretically. – A third variable, the *intermittency*, must also be taken into account during the measurement and simulation of frequencies so that the order of magnitude of the fluctuating concentration can be assessed and modelled properly.

Concept of the Experiments

In the past decades, numerous more or less extensive experimental examinations of the dispersion behaviour of airborne materials in the lower atmosphere (so-called dispersion experiments) were carried out with different objectives. The main goal of these examinations was the measurement of long-term mean values of concentration with emission heights of more than 20 m. Recently, increasing research activity in the area of the modelling and measurement of concentration fluctuations has been observed. This branch of research can roughly be divided into numerical simulation, physical modelling, and field experiments.

JONES [1] examined the concentration fluctuations of ionized air in the wake of an isolated building. However, it was only possible to take point measurements up to a distance of ca. 15 m. LEWELLEN and SYKES [2] published an analysis of the LIDAR measurements of fluctuating concentrations in plumes. DINAR [3] used oil fog as a tracer and was able to measure the concentrations with 30 Hz on the basis of optical detectors. The number of detectors was limited to 7 at a maximum source distance of 60 m. In a distance range of up to 1,000 m, MYLNE and MASON [4] were able to measure the concentration fluctuation of a propylene source with 10 Hz using a maximum of 10 detectors. A thorough analysis of the statistical properties of fluctuating concentrations was provided by YEE [5]. Once again, propylene was used as a tracer, whose concentrations were measured with 9 modified 100 Hz photoionization detectors in a distance range of up to 100 m. In all these experiments, the tracer was released close to the ground (< 5 m above the ground) while atmospheric stratification was mainly neutral to slightly unstable.

The trial concept, which uses the dispersion of radioactive isotopes to deduce the fluctuation behaviour of airborne material in the lowest layer of the atmosphere, was already developed several decades ago. In a paper from the year 1971, RAMSDELL and HINDS [6] addressed concentration fluctuations and peak value conditions in plumes from a ground-level continuous point source. In their examination, the radioactive isotope krypton-85 (^{85}Kr) was used as a tracer. ^{85}Kr is an artificially produced gas with a half life of 10.76 years. It decays through β-emission at a maximum energy of 0.67 MeV.

In contrast to the above-mentioned paper, a systematic examination of the tracer concentration for the mean value and fluctuation values in the lowest Prandtl layer up to a source distance of 100 m is planned here. An odourant is intended to be emitted simultaneously with the radioactive tracer and registered by test persons so that the connection between tracer exceedance frequencies and periods with odour perception can be described. The use of modern, highly sensitive planiform counting tubes allows the required rates of ^{85}Kr emission to be limited to a relatively low value. – At the Institute of Agricultural Engineering Potsdam-Bornim, the ^{85}Kr measuring technique has been successfully employed for years to measure the air-change rates of stall buildings [7]. When used for open-field immission measurements, it provides a decisive advantage over other measuring techniques: a *large number* of comparatively inexpensive detectors can be employed for *simultaneous* concentration measurement.

The temporal resolution of impulse rate measurement is determined by a sufficiently large signal/background ratio. This ratio is dependent upon the tracer concentration at the measuring point and is mainly determined by source strength, source distance, and the wind field. "Sufficiently" large signal/background ratios are provided by source strengths of 10 MBq/s, source distances of approximately 100 m, and average wind velocities of about 3 m/s at measurement rates of 1 s. Therefore, the temporal resolution of the tracer concentration measurement amounts to 1 s. It has deliberately been kept within the range of the reaction time (not breathing frequency!) of the human nose. It is not the objective of the present dispersion experiments to examine the small-scale inertial subrange and to analyze the energy spectra of the concentration fluctuations.

The concept of the present study follows an old scientific rule, which has often fallen into oblivion: "begin with the simplest things which are easiest to comprehend in order to climb gradually, so to speak stepwise, to the knowledge of those which are most complex"[1]. In the present study, this rule is applied by setting a group of conditions for the experiments:

- point sources
- sources of temporally constant emissions
- identical emission- and receptor heights
- source distances of 20 m, 50 m, and 100 m
- level terrain with uniform roughness length
- defined meteorological boundary conditions.

These restrictions fulfill the prerequisites for the examination of the statistical characteristics of the fluctuating tracer concentrations at different evolution stages of the dispersing tracer plume. Mainly due to the above-cited studies, a clearer picture of plume development has recently established itself, which also serves as a model in the present study. According to this model, the fluctuations of concentration must be attributed to a wide scale of turbulent movements in the plume, which in turn reflects the large bandwidth from the smallest to very extensive eddy structures. At an early stage of plume development, where the width of the momentary plume σ_0 is small as compared with the integral turbulence scale Λ of the eddy elements, the meandering of the plume, i.e. the large eddy structures, makes the main contribution to fluctuation. This phase can be distinguished from a stage where plume width ranges in the order of magnitude of the length scale of the turbulent eddies. Here, progressive deformation of the plume edges due to the entrainment of neutral ambient air into the plume becomes noticeable. When the plume spreads further, those eddies finally make a dominant contribution towards the fluctuation process whose extension is small as compared with plume width. This in-plume mixing of air parcels carrying airborne material with neutral ambient air leads to complex, non-Gaussian concentration distributions, whose measurement, analysis, and mathematical modelling is one objective of the present study.

In order to determine the connection between exposure and effect in the case of odour perception, the odourant tetrahydrothiophen (THT) is released during some open-field experiments simultaneously with the emission of ^{85}Kr. THT has the empirical formula C_4H_8S and, hence, a molecular weight of 88.168. The odour threshold value (limit of perceptibility) amounts to 13 μg/m^3 [9]. As an odourant, THT also meets the general requirements for an odour tracer, which should neither be toxic nor harmful in any other way, distinctive from other frequently occurring odours, chemically inert, thermally stable, and usable at low temperatures.

Experimental Set-Up and Measuring Instruments

An overview of the basic measurement set-up and initial results has already been

[1] Le troisième [règle], de conduire par ordre mes pensées, en commencant par les objets les plus simples et les plus aisés à connâitre, pour monter peu à peu, comme par degrés, jusques à la connaissance des plus composés; et supposant même de l´ordre entre ceux qui ne se précèdent point naturellement les uns les autres [8].

given in a previous paper [10]. On level terrain exposed to a free, largely undisturbed air flow (pasture land with ca. 0.2 to 0.3 m tall grass, mean roughness length $z_0 \cong 0.04$ m), the radioactive isotope ^{85}Kr is released from a plastic hose 1.9 m above the ground as a "point source". ^{85}Kr emission works according to the displacement principle: from a tank, a constant water flow is led into a 5 l gas bottle, which has been filled with ^{85}Kr of known quantity and activity before. In the bottle, the rising water level continuously presses the ^{85}Kr gas into the plastic hose. The volume flow is controlled by a suspended particle flowmeter (rotameter). Depending on the experiment, emission periods ranged between 9 min and 24 min. Atmospheric stratification was largely neutral to unstable.

On the lee side of a circle segment with an opening angle of ca. 60°, a total of 10 cylinder-shaped Geiger-Müller counter tubes (cylinder counter tubes) are mounted at a source distance of 50 m. 10 planiform proportional counter tubes (planiform counter tubes)[2] are installed on a second circle segment with the same opening angle at a source distance of 100 m. The height of the detection centre of all counter tubes is situated approximately at the emission level between 1.8 m and 1.9 m above the ground (**figure 1**).

Between the source and the counter tubes, the wind vector is measured using 2 ultrasonic anemometers at 2.5 m and 10 m above the ground. The wind gauge at a height of 2.5 m (approximately the level of emission) is a USA-1 ultrasonic anemometer from the METEK company, Hamburg, which records the 3 components of the wind vector with 10 Hz. For wind measurement at a height of 10 m, an ultrasonic anemometer from the British company Gill Instruments, Ltd., Lymington/Hampshire is employed (temporal resolution 1 s).

In all open-field tracer experiments, the measurement data of all counter tubes are transferred to a central computer using the aid of a wireless telemetric system and saved in 1 s intervals.

According to reference [11], a factor of 4,500 (impulses · min^{-1}) / (MBq · m^{-3}) is employed for the cylinder counter tubes used in order to convert the measured impulse rates into concentration units. As shown by series of comparative experiments in a closed room with a volume of ca. 100 m^3, the planiform counter tubes have a sensitivity ca. 17 times higher. During the subsequent evaluation of the experiments, a conversion factor of 76,500 (impulses · min^{-1}) / (MBq · m^{-3}) is therefore employed for the planiform counter tubes. For the rate of ^{85}Kr emission, the relative error can be estimated at < 10%.

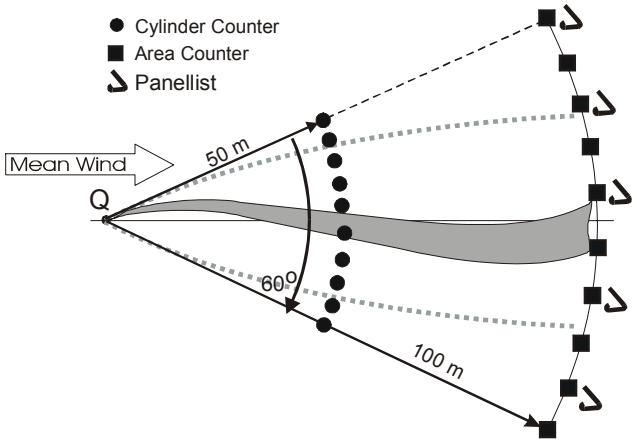

Figure 1: This diagram shows the arrangement of the Geiger-Müller counter tubes. The point Q marks the ^{85}Kr source and the THT source (in some experiments).

The Carrying Out of the Experiments

In the period from 28 June 2000 until 18 May 2001, a total of 9 dispersion experiments were carried out according to the described measurement arrangement. During the first 4 series of experiments, the cylinder counter tubes were placed at a downwind distance of 20 m, whereas the planiform counter tubes were installed at a distance of 50 m. For 5 other series of experiments, the distance was increased to 50 m and 100 m respectively. In the last 4 experiments, the odourant THT was additionally released in a defined manner at the same time and at the same location as the tracer ^{85}Kr. Depending on the day of the experiment, air temperatures changed between ca. 0°C and 20°C with varying degrees of coverage. At the anemometer height of 2.5 m above the ground, the wind velocities averaged out over the trial period ranged between 0.8 m/s and 5.2 m/s and thus covered a sufficiently large part of the wind velocity spectrum. Friction velocities allowed a mean roughness length of $z_0 \cong 0.04$ m to be deduced, which is remarkably consistent with the literature value for pasture land. The majority of the fluctuations of wind direction over individual periods of the experiments exhibit a strikingly irregular structure. For averaging periods of 15 – 30 min, wind directions show a normal Gaussian distribution approximately around the mean value. (During longer averaging periods, multi-Gaussian distributions for several superposed main wind directions may occur.) With regard to the low-frequency range, however, the so-called meandering (> 1 min), no clear periods can be detected. – **Table 1** provides a summarizing overview of the data of the dispersion experiments.

The odourant THT was released according to the principle of evaporation. In addition to the natural wind flow, a powerful PC fan mounted to a holder ca. 0.2 m above the Petri dish containing the odourant provided a higher evaporation air flow. The mass loss, i.e. the rate of THT emission, was determined with an electronic assay balance, on which the Petri dish was installed. Since, by approximation, the measurement showed a linear mass loss over time, the rate of emission can be determined immediately from the quotient of mass difference and corresponding time difference[3]. In all 4 dispersion experiments, source strength was in the order of 10 mg/s with an estimated relative error of 5%.

Without exception, sufficiently high impulse rates, i.e. a signal/background ratio large enough for evaluation, were measured by at least one counter tube in all series of experiments. **Figure 2** shows a typical recording of the impulse rates measured by a cylinder counter tube. (V6, pos. Z2. The uninterrupted line denotes the mean value of 2.2 imp./s. The peak/mean value ratio amounts to p/m = 37).

The "emission free pre-run" 2 to 3 minutes before the tracer was released allowed the radioactive radiation background to be determined. For the planiform counter tubes used, the mean values amounted to I_{HFI} = 11 impulses / s,

[2] In the first 4 of a total of 9 series of experiments, source distances amounted to 20 m and 50 m with 10 counter tubes on each arc segment. Due to the significant fluctuations in the wind direction, two additional adjacent counter tubes each were installed during the last two series of experiments (with a source distance of 50 m and 100 m). This resulted in a wider segment with 12 cylinder counter tubes and 12 planiform counter tubes.

[3] In the series of experiments V5 and V6, the Petri dish had a diameter of ∅ = 0.145 m. In the series of experiments V7 and V8, ∅ was 0.185 m. Mass loss variations are caused by natural wind fluctuations. All measurement values were saved at time intervals of 10 s. – The rate of emission is mainly determined by the effective THT surface, i.e. the diameter of the Petri dish and the strength of the air flow. To a lesser extent, it is also determined by air temperature, humidity, and other parameters.

Table 1: Overview of the data from the 9 series of experiments

Exp.	Date	Emission period	Q_{85Kr} [MBq/s]	D [^{0}]	V [m/s]	u* [m/s]	σ_v [m/s]	σ_w [m/s]	t [^{0}C]	Q_{THT} [mg/s]	d [m]	DC
V0	28.06.00	15:07 – 15:19	7.5	280	5.13	0.462	1.05	0.487	13.8	-	20/50	7/8
V1	04.10.00	14:20 – 14:38	5.0	170	1.49	0.234	0.909	0.348	19.4	-	20/50	1/8
V2	05.10.00	14:20 – 14:36	5.6	363	0.801	0.053	0.442	0.146	18.3	-	20/50	6/8
V3	05.10.00	15:13 – 15:29	5.6	314	0.839	0.078	0.560	0.149	18.7	-	20/50	6/8
V4	05.10.00	16:52 – 17:01	9.7	282	1.37	0.125	0.167	0.111	18.5	-	50/100	5/8
V5	27.03.01	14:51 – 15:15	6.4	117	3.54	0.326	0.963	0.402	1.62	4.7	50/100	2/8
V6	27.03.01	16:16 – 16:28	12.5	134	2.66	0.268	0.688	0.361	2.13	6.1	50/100	2/8
V7	18.05.01	11:53 – 12:10	9.7	256	3.78	0.433	1.26	0.492	15.8	22	50/100	1/8
V8	18.05.01	13:14 – 13:30	10.6	275	3.63	0.418	1.21	0.499	15.4	13	50/100	1/8

Rates of emission Q, mean wind direction D and wind velocity V at 2.5 m above the ground, friction velocity u*, standard deviations σ_v and σ_w of the wind velocity components v and w, air temperature t, source distance of the counter tubes d (cylinder-/planiform counter tubes), degree of sky coverage DC

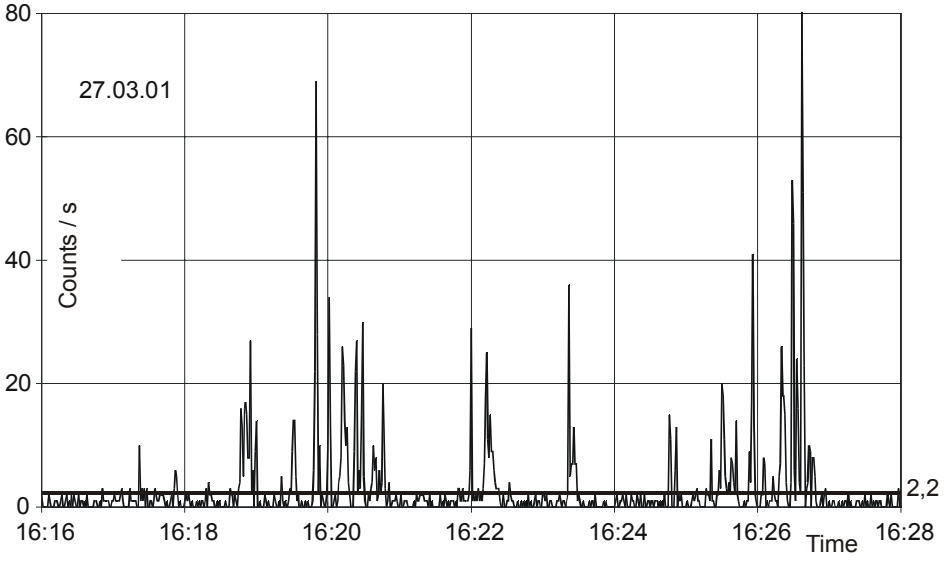

Figure 2: Typical example of impulse rates measured at a source distance of 50 m

whereas in the cylinder counter tubes the *statistical average* of the mean impulse rates for the background was significantly lower at I_{HZy} = 0.65 impulses/s. The standard deviation for the background impulse rate of the planiform counter tubes amounts to σ_{HFI} = 3.3 imp./s. For the calculation of the mean values and exceedance frequencies from the measured time series of the impulse rates, the measurement values are corrected by the individual background value.

In some cases, the peak values of the impulse rates were more than 2 orders of magnitude above the mean value. In principle, p/m is dependent upon the ratio of the sampling frequency and the averaging time (here: approximately 1 s : 1,000 s), the source distance, and the position of the measuring point in relation to the tracer plume axis. In addition, dependence upon the extension of the source σ_0, atmospheric turbulence, and other influencing factors is observed. In paragraph 5.1, the measured values for p/m are discussed coherently and examined in more detail.

Analysis of the Measurement Results

As expected, those counter tubes which, seen from the source, are closest to the mean wind direction, show the highest impulse rates. For this reason, they are used as reference points for the plume axis. **Table 2** lists the mean values of the measured tracer concentrations for these reference points (plume axis) as well as the adjacent measuring points (counter tube positions) on the left and the right side[4].

The measurement values are compared with the results of corresponding dispersion simulations. Here, the (simplified) Gaussian plume equation serves as a dispersion model:

$$C(x,y) = \frac{Q}{2 \cdot \pi \cdot \bar{u} \cdot \sigma_Y(x) \cdot \sigma_Z(x)} \cdot \exp\left\{-\frac{y^2}{2 \cdot \sigma_Y{}^2(x)}\right\} \cdot \left[1 + \exp\left\{-\frac{8}{\sigma_Z{}^2(x)}\right\}\right] \quad (1)$$

Q - source strength,
$\bar{u}$ - mean wind velocity at transport height,
σ_y and σ_z - horizontal and vertical dispersion parameter,
x and y - coordinates of the receptor point (The coordinate z was eliminated through z = h = 2 m.)

Two different approaches for the dispersion parameters must be examined:

First, according to Taylor´s theorem [12], the term eq. (2) is used, which is strictly valid if turbulence is assumed to be homogeneous, at least for those three limit cases where the dispersion time t is short, approximately identical, and long as compared with the Lagrangian time scale T_L. For illustration, the Lagrangian time scale can be termed a measure of the "memory of an air parcel" of its previous state of motion. In figures, it shows how strongly the velocity fluctuations at two different moments and at one location are correlated.

$$\sigma_{y,z}(x) = \frac{\sigma_{v,w} \cdot t(x)}{\sqrt{1 + t(x)/(2 \cdot T_{Ly,z})}} \quad (2)$$

with
t(x) - dispersion time (simplified: $t(x) = x/\bar{u}$)

The standard deviations of the wind velocity components σ_v and σ_w immediately result from the wind measurements (cf. table 1), whereas the determination of the Lagrangian time scale T_L meets with sig-

[4] Distance between the counter tubes results from the source distance listed in Table 1 and the angle segment. For the source distance of 20 m, it amounted to d = 2.4 m. For source distances of 50 m and 100 m, distance between the counter tubes was 5.8 m and 11.7 m respectively.

Table 2: Measured ($\overline{C}_M$) and calculated ($\overline{C}_R$) mean tracer concentrations from the 9 series of experiments

Exp.	$\overline{C}_M$ [kBq/m³]		$\overline{C}_{R2}$ [kBq/m³]		$\overline{C}_{R3}$ [kBq/m³]	
	•	□	•	□	•	□
V0	34,7	10.8	29.6	8.02	15.2	4.16
	42.6	**12.6**	**35.7**	**9.79**	**16.2**	**4.55**
	28.5	12.4	29.6	8.02	15.2	4.16
V1	8.6	1.6	19.7	5.06	21.9	4.66
	13.4	**4.8**	**20.2**	**5.23**	**22.5**	**4.83**
	11.7	1.6	19.7	5.06	21.9	4.66
V2	18.9	1.2	59.5	19.1	45.6	9.71
	25.1	**3.4**	**61.8**	**20.2**	**46.8**	**10.1**
	22.9	2.3	59.5	19.1	45.6	9.71
V3	30.1	4.0	47.5	15.3	43.5	9.27
	36.9	**6.7**	**48.8**	**15.9**	**44.7**	**9.61**
	23.0	3.4	47.5	15.3	43.5	9.27
V4	37.9	13.8	51.2	15.0	22.2	8.08
	120.3	**45.1**	**122**	**55.1**	**23.8**	**8.96**
	38.7	-	51.2	15.0	22.2	8.08
V5	8.7	1.2	7.64	2.58	4.02	1.18
	10.5	**1.5**	**8.64**	**3.02**	**4.31**	**1.29**
	6.2	1.4	7.64	2.58	4.02	1.18
V6	-	4.6	19.2	6.50	6.52	1.75
	28.2	**5.0**	**22.2**	**7.93**	**6.76**	**1.83**
	9.5	4.3	19.2	6.50	6.52	1.75
V7	12.3	3.4	8.22	2.72	3.56	0.955
	12.5	**4.5**	**8.91**	**3.01**	**3.69**	**1.00**
	9.4	2.5	8.22	2.72	3.56	0.955
V8	6.1	1.7	9.03	2.98	4.05	1.09
	7.7	**2.5**	**9.80**	**3.31**	**4.20**	**1.14**
	5.2	1.7	9.03	2.98	4.05	1.09

• cylinder counter tubes / □ planiform counter tubes. $\overline{C}_{R2}$: values calculated according to eq. (2), $\overline{C}_{R3}$: values calculated according to eq. (3). The middle series of numbers (in bold print) stands for the counter tube position with maximum concentration (plume axis). The values above refer to the neighbouring counter tube position to the left in wind direction. The values below refer to the position on the right side.

nificant difficulties in practice. For (slightly) unstable atmospheric stratification and a mean transport height of approximately 3 m above the ground, it is assumed here that $T_L = 20$ s. (No distinction is made between the vertical and the horizontal component, i.e. $T_{Ly} = T_{Lz}$). The dispersion times of the tracer from the source to the detectors are in the order of this value. Given an assumed uncertainty of $T_L = 20$ s ± 10 s, the relative error in the dispersion parameters according to eq. (2) thus remains below 14%. Therefore, the Lagrangian time scale is no critical influencing variable for dispersion times $t \leq T_L$. Only if dispersion times are long ($t >> T_L$) does its influence on the calculation of the dispersion parameters become dominant.

Second, the dispersion parameters are calculated according to the general administrative regulation of the Federal Ambient Pollution Control Act, the Technical Regulations Concerning Air Pollution [13]. (Values for F, G, f, and g can be gathered from the Appendix C, N° 10 c of the Technical Regulations Concerning Air Pollution.)

$$\sigma_Y = F \cdot x^f \qquad \sigma_Z = G \cdot x^g \qquad (3)$$

The Gaussian model provides statistical information about mean concentration at the receptor point. This means that only a larger number of measurement values – pooled in a mean value – can be compared with *one* calculation result. Since the meteorological boundary conditions in open-field experiments are not repeatable, the dispersion experiments cannot be reproduced, i.e. a larger number of measurement values for constant boundary conditions cannot be generated. Nevertheless, a comparison of calculation and measurement is possible if a large number of measurement results from *different* series of experiments are considered as statistical values. At least, tendencies in the correlation diagram can be detected which enable the quality of the results of different model approaches to be evaluated. In **Figure 3**, the circles stand for the cylinder counter tubes, whereas the squares refer to the planiform counter tubes. Filled symbols represent the calculation results R2 according to eq. (2). Empty symbols stand for the calculation results R3 according to eq. (3).

If one ignores the series of experiments V2 (set off through a broken frame in Figure 3), where with great likelihood the concentration maximum was missed during measurement, the model according to eq. 2 on the whole describes the measured values better than the model equation (3). Parameterization according to eq. (3) generally leads to an underestimation of mean concentration. This is caused by the composition of the data set of the Technical Regulations Concerning Air Pollution, which is only valid for source heights > 50 m. Especially since, according to the Technical Regulations Concerning Air Pollution, the dispersion categories are divided into only 6 classes, extreme calculation errors may occur in some cases. In the series of experiments V4, for example, the measurement value is underestimated by the 5-fold amount (!) (not shown in Figure 3 for scale reasons; cf. table 2). For the mentioned reasons, the model eq. (3) is not suitable for the *diagnosis* of ambient air concentrations. It may be applicable for the *prediction* of

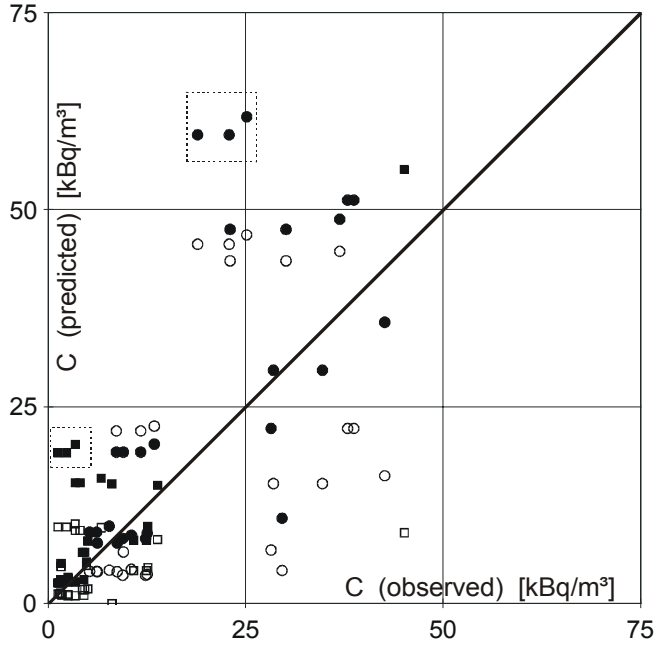

Figure 3: Correlation diagram of the measured and calculated mean tracer concentrations in kBq/m^3 according to Table 2.

annual immission because in this case some (random) errors average each other out and the statistical accuracy of prediction is mainly determined by the meteorological statistics or time series which form its basis.

Peak Values of Tracer Concentration and Intermittency Rates

The evaluation of the unfiltered concentration time series[5] shows that the peak-to-mean conditions p/m are scattered over almost 2 orders of magnitude ($4 < p/m < 99$ at the counter tube positions listed in Table 2). Conditioned concentrations, i.e. time series with filtered-out zero concentrations, result in smaller p/m quotients due to higher mean values. In this case, the peak-to-mean ratio only changes by one order of magnitude ($3 < p/m < 30$). Moreover, the connection between p/m and fluctuation intensity i^2 is examined, which is defined as

$$i^2 = \frac{\sigma_c^2}{\overline{C}^2} \qquad (4)$$

with

$\overline{C}$ - as the mean value

σ_c^2 - as the variance of concentration.

Unfiltered time series – as shown in **Figure 4** - and conditioned ones exhibit a linear connection between p/m and i^2:

$$p/m = 1 + \alpha \cdot i^2 \qquad (5)$$

The factor was determined to be $\alpha = 3.6$. (For $i^2 = 0$, i.e. no fluctuation of concentration, the peak value cannot be higher than the mean value, i.e. p/m=1 for i^2=0.)

The intermittency rate μ is defined as the part of a time series where the concentration values are different from zero, i.e. exceed a minimum concentration C_{min}. The definition of C_{min} is slightly arbitrary. In physical measurements, the detection limit of the measuring instrument used generally serves as a point of orientation. Due to the fluctuating radioactive background radiation, C_{min} cannot simply be equated with the detection limit of the counter tubes in the present case. C_{min} and I_{min} are chosen such that during the emission-free pre-run of a time series μ remains < 0.02 (cylinder counter tubes I_{min} = 1 imp./s and planiform counter tubes I_{min} = 3 imp./s, σI_{HFI} = 3.3 imp./s, cf. paragraph 4).

According to Figure 1, the tracer concentrations were measured *simultaneously* at 2 different source distances in all field experiments. Without exception, a reduction of the peak-to-mean ratio (and, hence, also of fluctuation intensity) was observed in all 9 series of experiments as distance from the source increased. Intermittency, as defined above, however, increases with growing distance. This process (reduction of p/m and i^2 and a simultaneous increase in μ with growing source distance) is a consequence of the increasing mixing of "tracer/air parcels" with neutral ambient air. With growing distance from the source, plume meandering also makes a smaller contribution towards the fluctuation of concentration. At the beginning, a turbulent-convective regime develops ($t \cong T_L$). Larger eddies, which cause meandering, make approximately the same contribution towards fluctuations as the small-scale eddy structures, which lead to internal mixing and to the expansion of the plume.

After longer dispersion times ($t >> T_L$), a turbulent-dispersive regime evolves in plume dispersion. In this case, concentration fluctuations are mainly caused by small-scale, in-plume eddy elements. At this stage, uniform mixing of the air volumina laden with airborne material and neutral ambient air becomes noticeable. The plume is "well mixed" and develops in a self-similar way with relatively small concentration gradients, i.e. low values for p/m. This is only mentioned for the sake of completeness. In our measurements, dispersion times were in the short to medium range ($t \leq T_L$).

Measured Frequency Distributions

Below, the measured exceedance frequencies in the tracer plume (conditioned time series) are considered in more detail. The concentrations were normalized with

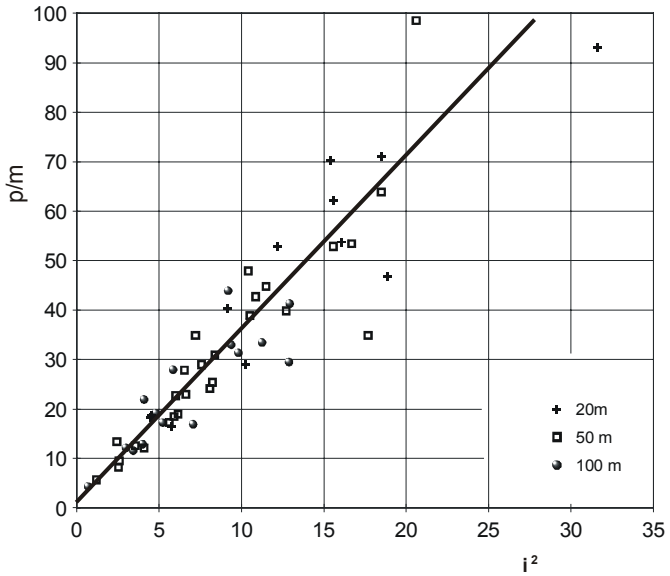

Figure 4: Peak-to-mean ratio p/m over fluctuation intensity i^2 for the position next to the plume axis and the two adjacent counter tube positions. Unfiltered (total) concentration time series from all 9 series of experiments.

[5] Time series where only the individual background concentration was subtracted from the measured impulse rate are termed "unfiltered" time series, i.e. the periods with zero concentration are not filtered out.

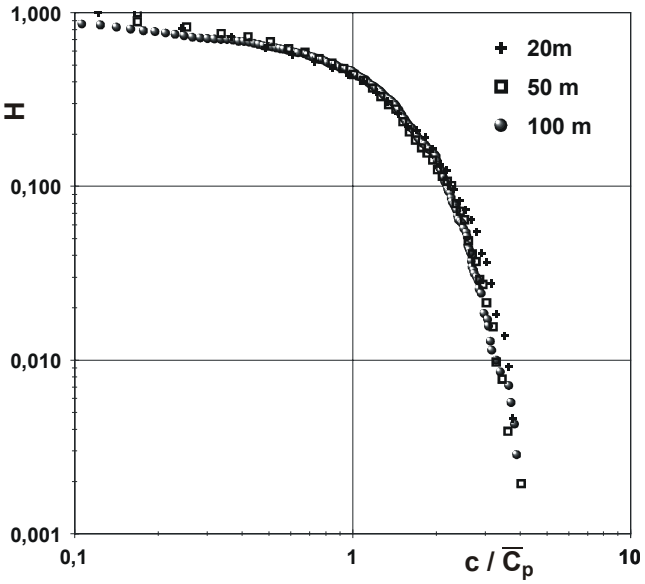

Figure 5: Exceedance frequencies H for conditioned-normalized concentrations $c/\overline{C}_p$, measured at 3 different source distances in the plume centre (V1: 20 m, V4: 50 m / 100 m).

their mean value and thus made dimensionless so that the time series from different dispersion experiments could be compared better. If one sorts the conditioned-normalized concentration values and establishes the fraction of the data points which exceed predetermined values $c/\overline{C}_P$, one obtains the exceedance frequencies shown in **Figure 5**. According to these results, peak values larger than the 3.5-fold amount of the mean value (p/m > 3.5) are only reached with a frequency of 1% in the centre of the plume. The other series of experiments provide comparable values and show strikingly self-similar (exceedance-) frequency distributions for different source distances.

The values of (concentration-) distribution with the highest probability are termed modes. In pronounced right skewed distributions, as in the present case, the mode is always smaller than the mean value. The difference between the two values is a measure of the degree of skewness. If one considers the edge of the tracer plume, the modes of the measured concentrations amount to ca. 10% of the mean value. In the centre of the plume, modes of approximately 50% of the mean value are observed. The heavy asymmetry in the frequency distribution of the measured concentrations with a long, quasi-exponential tail on the right side is caused by high concentrations in locally unmixed tracer spots.

Modelling of the Exceedance Frequencies

The total distribution function for the probability of occurrence of atmospheric material at a receptor point is given by

$$F_t(c) = \mu \cdot F(c) + (1-\mu) \cdot H(c) \qquad (6)$$

H(c) is the unit step function at c = 0.

If the differential is derived for the concentration c, the term eq. 6 provides the total probability density function (pdf):

$$p_t(c) = \mu \cdot p(c) + (1-\mu) \cdot \delta(c) \qquad (7)$$

with
δ(c) - Dirac delta function.

If the intermittency rate μ is known, the total pdf is consequently determined entirely by density function p(c). Below, 3 pdfs frequently used for the modelling of concentration data are tested:

Gamma distribution

$$p(c) = \left(c/a\right)^{b-1} \cdot \frac{\exp(-c/a)}{a \cdot \Gamma(b)} \qquad (8)$$

Logarithmic normal distribution

$$p(c) = \frac{1}{\sqrt{2\pi} \cdot c \cdot b} \cdot \exp\left\{-\frac{\ln^2(c/a)}{2 \cdot b^2}\right\} \qquad (9)$$

Weibull distribution

$$p(c) = \frac{b}{a} \cdot \left(\frac{c}{a}\right)^{b-1} \cdot \exp\left\{-(c/a)^b\right\} \qquad (10)$$

with
a - scale parameter
b - shape parameter.

Apart from the 2nd moment, variance according to eq. (4), the 3rd and 4th moment are characteristic of the fluctuation properties of a concentration time series:

skewness:

$$S = \frac{\overline{(c-\overline{C})^3}}{\sigma_c^3} \qquad (11)$$

kurtosis:

$$K = \frac{\overline{(c-\overline{C})^4}}{\sigma_c^4} \qquad (12)$$

with
$\overline{C}$ - as the mean value
σ_c^2 - as the variance of concentration.

The connection between skewness and kurtosis as well as the scale- and shape parameters of the above-mentioned pdfs is obtained by putting p(c) into the definition equation of the statistic moment and through subsequent integration. S and K follow as functions of the shape parameter b, which in turn is exclusively dependent upon fluctuation intensity i^2 (cf. reference [14], for example). On the other hand, i^2 can also easily be derived from the measurement data using eq. (4).

In the following two diagrams (**figure 6 and figure 7**), skewness and kurtosis are plotted over fluctuation intensity i^2 in order to examine how well the 3 pdfs describe the fluctuation-statistical properties of the measured concentration values. For this comparison, the measurement data from all 9 series of experiments are employed. They refer to conditioned time series at the counter tube positions listed in Table 2.

According to the above-shown diagrams, LogNormal distribution provides the least accurate description of the measurement data. It forms an upper limit for the 3rd and 4th statistical moment, i.e. the measurement values for S and K do not exceed the curves of LogNormal distribution. On the whole, the measured statistical moments are best described by gamma distribution. Due to the widely scattered atmospheric conditions and the different relative plume positions, however, they rather tend to form a plane than a curve in the (S,i^2)- or (K,i^2) plane. These results are largely identical with the examination results of YEE et al. [5].

The comparison of calculated and observed *exceedance frequencies* is the most important test for the validation of a density function. Such a comparison immediately shows how well the model simulates the actual exceedance frequencies. Therefore, the form of representation chosen is a quantile-quantile diagram, which shows the exceedance frequency as a function of the threshold value. The quantile of the normalized measurement values $(c/\overline{c})_M$ and that of the model simulation $(c/\overline{c})_R$ for a source distance of 100 m are plotted on the abscissa and the ordinate respectively. (The Q-Q diagrams

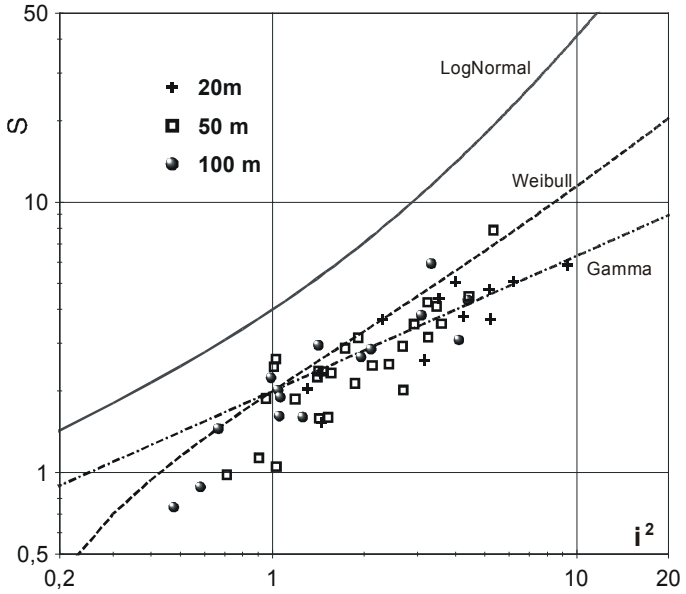

Figure 6: Skewness S of the measured tracer concentrations over fluctuation intensity i^2 for 3 different source distances. Comparison with 3 statistical density distributions.

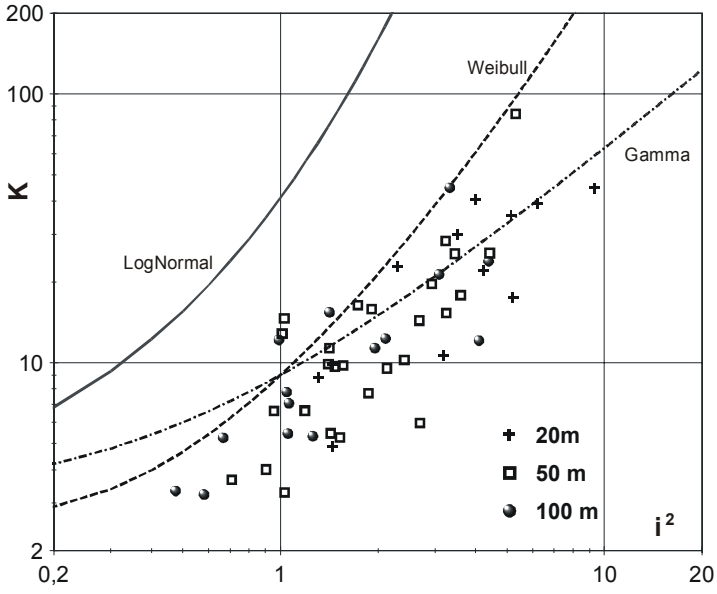

Figure 7: Kurtosis K of the measured tracer concentrations over fluctuation intensity i^2 for 3 different source distances. Comparison with 3 statistical density distributions.

for source distances of 20 m and 50 m are not significantly different from **Figure 8**). Gamma- and Weibull distribution provide rather similar Q-Q profiles, which on the whole match the observed quantiles better than the Q-Q profile of LogNormal distribution. At least at the edge of the tracer plume, however, gamma- and Weibull distribution underestimate the quantiles in small concentrations, whereas they slightly overestimate them in higher concentrations. By contrast, the calculated quantiles of LogNormal distribution constantly range above the observed values. As in the case of the *measured* frequency distributions, the modes of the density functions are significantly lower than the mean value of concentration. Gamma- and Weibull distribution underestimate the modes in *smaller concentrations*, whereas in this case LogNormal distribution represents the most frequent measurement value of concentration better.

Dispersion simulations generally yield (long-term) mean values of concentration. These values contain periods with zero concentration, which can no longer be identified, and provide no information about intermittency. If one equates $\mu = 1$ (which equals "no information about intermittency") in the model simulation and calculates the model parameters a and b from the mean value and the fluctuation intensity of the measurement values again, calculated and measured exceedance frequencies for certain threshold values can be listed in an H-H diagram, which provides an illustrative comparison (**figure 9**). Not only the calculated Hr and the measured exceedance frequency Hm are dependent upon the threshold value of the concentration C_0, but also the quotient Hr/Hm generally depends on the choice of the value C_0. For calculation and representation in Figure 9, the threshold value is equated with the mean value of concentration $C_0 = \overline{C}$ (with a certain arbitrari-

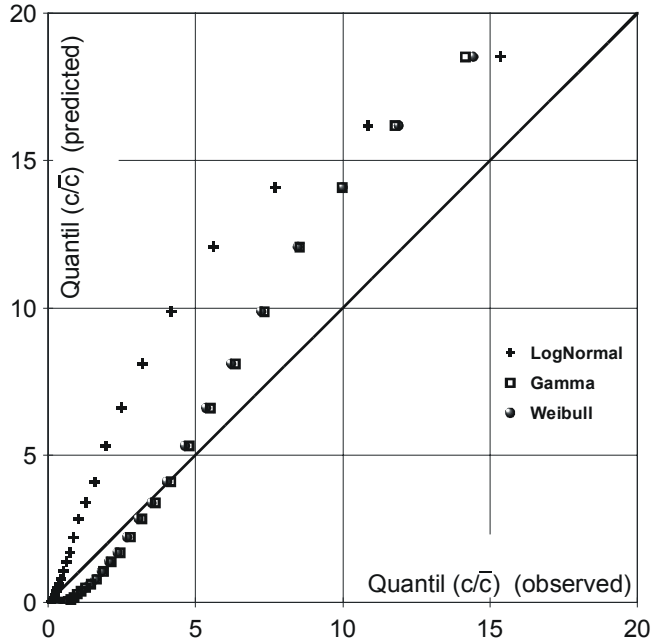

Figure 8: Quantiles of the normalized concentrations in the plume axis at a source distance of 100 m in comparison of model simulation and observation. The model parameters a and b were calculated from the mean value and the fluctuation intensity of the measurement values.

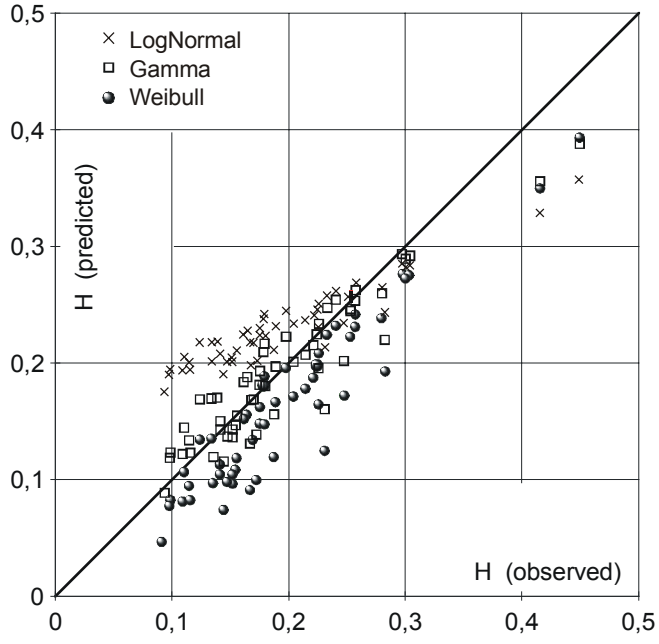

Figure 9: Exceedance frequencies H for unfiltered concentrations (original data) in a comparison of measurement and calculation. In the model calculations with the 3 density functions, μ was equated with 1; $C_0 = \overline{C}$.

ness) because the following relation applies to most evaluated time series: $C_{min} << \overline{C} << C_{max}$. Below, the mean square deviation of the quotient of calculated and measured exceedance frequency serves as a measure of the deviation between calculation and measurement:

$$\sigma_{Hr/m} = \sqrt{1/n \cdot \sum_{i=1}^{n} (H_{ri} / H_{mi} - 1)^2} \qquad (13)$$

According to Figure 9, gamma distribution represents the observed exceedance frequencies remarkably well not only in comparison with the two other density functions, but also if considered absolutely. Even if the threshold value $C_0 = 3 \cdot \overline{C}$ or concentrations are 3 times higher, a high degree of consistency with $\sigma H_{r/m} = 0.189$ can still be established. For $C_0 = 1/3 \cdot \overline{C}$, standard deviation is $\sigma H_{r/m} = 0.246$.

Among other factors, the high degree of consistency in the H-H diagram above must be attributed to the following condition: with $\mu = 1$, the calculated exceedance frequencies may be overestimated, but at the same time they are reduced by the mean value of concentration, which is lower for unfiltered time series. These opposing tendencies partly cancel each other out. Thus, practical relevance is given because concentrations of airborne material in the atmosphere usually are *not* measured with high temporal resolution.

This is different in the case of fluctuation intensity i^2. As shape parameter b, it is a decisive factor for model simulation. Together with the mean value of concentration, it thus significantly determines exceedance frequency. The comparison in Figure 9 is therefore strongly dependent upon the fluctuation intensity i^2 of the individual series of experiments, which can only be established through measurement techniques with high temporal resolution. This allows the following conclusion to be drawn: as compared with fluctuation intensity, intermittency is the less critical influencing factor because μ is implicitly contained in the mean value, while i^2 proves to be largely independent of the mean value. (Of course, this only applies to the calculation of exceedance frequencies with the introduced density functions. It does not mean that intermittency can be deduced from the mean value!)

Correlation between Tracer Concentration and Odour Perception

In principle, the THT-odours can be perceived without any doubt even at larger distances of 100 m and above. In some cases, the sensory perception patterns of the panellists exhibit a high degree of coincidence with the exceedance patterns of tracer concentration at the same measuring point (**figure 10**). However, data basis of the measured THT series is not sufficient in order to calculate correlation coefficients of exposure (immission) and odour effect. Thus, the following presentation of results can only provide orientation.

If one compares the observed odour frequencies with pure model simulations, the series of experiments V7 and V8 show deviations by approximately a factor of 2 (cf. **Figure 11**; a significantly larger deviation was established in the series of experiments V6.) In this case, "pure model simulations" means: in contrast to the comparison according to Figure 9, the mean value of concentration was not gained through measurement, but calculated according to equations (1) and (2) (Q_{THT} according to Table 1 and C_0 = 1 OU/m^3). Only the value for i^2 was taken over into the model simulation from the corresponding series of measurements because no sufficiently accurate model for its determination has been available so far. (Model *approaches* can be found in reference [15], for example.)

The parallel experiments presented here pursued the objective of showing that THT is an appropriate odourant tracer which can be clearly "detected" by the panellists at distances of several hundred meters. The THT exceedance patterns established through sensory measurements can be compared with those for the tracer ^{85}Kr and evaluated. However, the connection between the exposure of odour concentrations and their effect cannot be quantitatively determined through a few field experiments. This applies even more if not only the registration of odour perception periods is intended, but also the determination of intensities, hedonic effects, and degrees of nuisance. With hedonic characteristics and nuisance, the connection between exposure and effect also comprises elements which are largely dependent upon sensation and can only be processed using the law of large numbers, i.e. by measure and number in statistical terms. The scientifically founded establishment of odour *effects* is also hindered

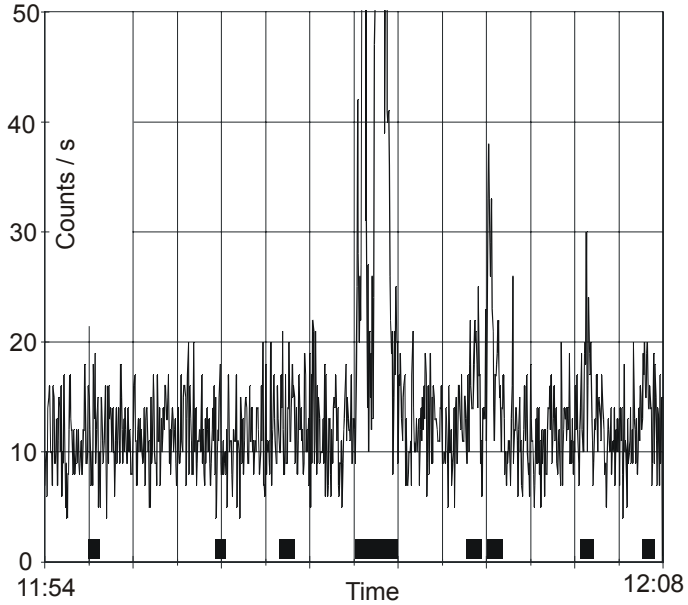

Figure 10: Measured impulse rates at a source distance of 100 m (V7, 18 May 01). The broken, bold line right above the abscissa shows the periods of odour perception registered by the panellist.

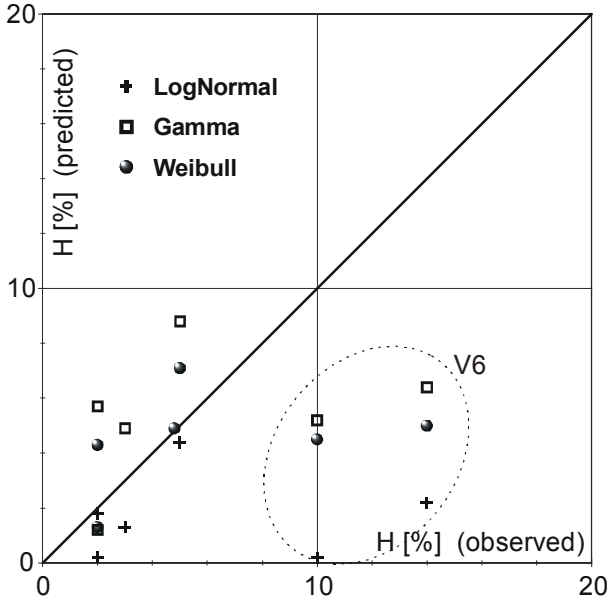

Figure 11: Calculated and measured exceedance frequencies H from the series of experiments V6, V7, and V8. The data points from V6 are circled with a broken line).

by other obstacles: most malodours are complex agglomerates of single odour substances, which means that the examination of a single component cannot simply be applied to a mixture of different odours. In practice, however, mixtures are the rule. In addition, the effects of odours with the same mean odour concentration under laboratory conditions at the olfactometer are different from those of fluctuating full-scale concentrations.

Summary

The present paper presents a measurement set-up for the determination of the immissions of the radioactive tracer ^{85}Kr. Among other detectors, highly sensitive proportional counter tubes are used, which allow a temporal resolution of 1 s to be achieved at relatively low krypton emission rates. Average ^{85}Kr emission amounts to 7.22 GBq per experiment at typical source distances of ca. 100 m. For the analysis of concentration fluctuations, a total of 9 open-field experiments were carried out on level terrain under the conditions of largely neutral to slightly unstable atmospheric stratification. The mean krypton concentrations were measured at source distances of 20 m, 50 m, and 100 m and compared with calculation results of the Gaussian plume model. These experiments showed that the parameterization of the standard deviations according to the Technical Regulations Concerning Air Pollution, Appendix C, generally underestimates the observed concentrations. If, however, one chooses a parameterization approach according to the TAYLOR theorem, which directly uses the wind velocity fluctuations $\sigma_{v,w}$, a higher degree of consistency with measurement can be established even with orientation values for the Lagrangian time scale T_L.

The ratio of the peak value to the mean value, i.e. p/m, of the measured unfiltered concentration time series varies over 2 orders of magnitude and may even reach values of p/m > 100 in the marginal area of the plume. A linear connection between p/m and fluctuation intensity i^2 can be proven. In addition, all dispersion experiments show a reduction of p/m and an increase in intermittency μ with growing source distance. The frequency distribution of the measured tracer concentrations shows a pronounced right skewness with modes of approximately 10% of the mean value for the edge and about 50% of the mean value for the centre of the tracer plume.

The statistical properties of logarithmic normal distribution, gamma-, and Weibull distribution are examined and compared with the corresponding values of the measured time series. Within the range of variation, gamma distribution, followed by Weibull distribution, reproduces the skewness and kurtosis of the measured values with sufficient precision, while LogNormal distribution significantly overestimates both statistical moments.

For a comparison of the calculated and the observed exceedance frequencies, the quantiles of the normalized calculation- and measurement values are formed and compared. Gamma- and Weibull distribution provide rather similar Q-Q profiles, which, as compared with those of Log-Normal distribution, on the whole show a higher degree of consistency with the observed quantiles. However, the two first-mentioned density functions underestimate the quantiles at small concentrations and slightly overestimate them at higher concentrations. Finally, in the H-H diagram, the calculated exceedance frequencies for $\mu = 1$ are compared with the unfiltered measured time series of concentration (which, hence, also contain periods with zero concentration) for a threshold value of $C_0 = \overline{C}$. As compared with the two other candidates, gamma distribution shows the highest degree of consistency with the measurement values. The results do not change significantly if the threshold value is altered within $\overline{C}/3 < C_0 < 3 \cdot \overline{C}$.

The dispersion experiments with the odorant tetrahydrothiophen (THT) provided the following result: under average wind conditions and at an emission rate in the order of 10 mg/s, the panellists perceive the THT odours without any doubt at a distance of 100 m. In some cases, the sensory perception patterns show a high degree of coincidence with the exceedance patterns of the tracer concentration at the same measuring point. However, the collected data basis is too small for correlations between the two exceedance patterns to be determined. With the examined density functions, dispersion calculations with the Gaussian model in the above-mentioned TAYLOR parameterization exhibit deviations by a factor of at least 2 as compared with the THT exceedance frequencies determined through sensory measurement.

References

[1] Jones, C. D., Griffiths, R. F. (1984) Full-scale experiments on dispersion around an isolated building using an ionized air tracer technique with very short averaging time, Atmos. Envir. 18, 903-916

[2] Lewellen, W. S. and Sykes, R. I. (1986) Analysis of concentration fluctuations from LIDAR observations of atmospheric plumes. J. Clim and Appl. Meteorol. 25, 1145-1154

[3] Dinar, N.,Kaplan, H. and Kleiman, M (1988) Characterization of concentration fluctuations of a surface plume in a neutral boundary layer. Boundary-Layer Met. 45 , 157

[4] Mylne, K. R. and Mason, P. J. (1991) Concentration fluctuation measurements in a dispersing plume at a range of up to 1000 m. Quart. J. Roy. Met. Soc. 117 , 177

[5] Yee, E.; Kosteniuk, P. R.; Chandler, G. M.; Biltoft, C. A. und Bowers, J. F. (1993) Statistical characteristics of concentration fluctuation in dispersing plumes in the atmospheric surface layer. Boundary-Layer Meteorology 65, 69-109

[6] Ramsdell, J. V. und Hinds, W. T. (1971) Concentration fluctuations and peak-to-mean concentration ratios in plumes from a ground-level continous point source. Atmos. Envir. 5, 483-495

[7] Müller, H.-J., Krause, K.-H. und Eckhof, W. (1996) Untersuchungen zum Emissions- und Immissionsverhalten von Puten- und Entenställen. Agrartechnische Forschung 2, H. 2, 127-137

[8] Descartes, R. (1637) Discours de la Méthode. Zitiert nach: Felix Meiner Verlag Hamburg 1960. 30

[9] DVGW Arbeitsblatt G 280 (1999) Technische Regel Arbeitsblatt G 280 - Gasodorierung. Wirtschafts- und Verlagsgesellschaft Gas und Wasser mbH, Bonn.

[10] Lung, T., Müller, H.-J., Möller,B. und Gläser, M. (2000) Messung und Modellierung von Konzentrationsfluktuationen für Gerüche. KTBL Sonderveröffentlichung zum KTBL/FAL-Fachgespräch, 24./25.10.2000. Braunschweig, Nr. 031 52-59

[11] Gläser, M.; Klich, W. und Creifelds, A. (1986) Vergleichende Untersuchungen an 85Kr und 133Xe als Tracer. Isotopenpraxis 22, 411-416

[12] Taylor, G. I. (1921) Diffusion by continuous movements. Proc. London Math. Soc. Ser. 2, 20, 196

[13] TA Luft (1986) Erste allgemeine Verwaltungsvorschrift zum Bundes-Immissionsschutzgesetz – Technische Anleitung zur Reinhaltung der Luft (TA Luft), GMBl. Nr. 7 vom 28.02.1986

[14] Yee, E.; Wilson, D. J.; Zelt, B. W. (1993) Probability distribution of concentration fluctuation of a weakly diffusive passive plume in a turbulent boundary layer. Boundary-Layer Meteorology 64, 321-354

[15] Hanna, S. R. (1984) Concentration fluctuations in a smoke plume. Atmos. Envir. 18, No. 6, 1091-1106

Authors

Dipl.-Phys. Thomas Lung
Ingenieurbüro für Immissionsprognostik
und Ausbreitungsmodellierung
10587 Berlin
E-mail: lung@snafu.de

Dr.-Ing. Hans-Joachim Müller
Institut für Agrartechnik Bornim e. V.
Abteilung Technik in der Tierhaltung
Max-Eyth-Allee 100
14469 Potsdam
Tel.: +49/(0)331/5699-518
Fax: +49/(0)331/5699-849
E-mail: hmuller@atb-potsdam.de

Dr. Manfred Gläser
Dr.-Ing. Hans-Joachim Müller
Institut für Agrartechnik Bornim e. V.
Abteilung Technik in der Tierhaltung
Max-Eyth-Allee 100
14469 Potsdam
Tel.: +49/(0)331/5699-518
Fax: +49/(0)331/5699-849
E-mail: mglaeser@atb-potsdam.de

Dipl.-Ing. Bernd Möller
Institut für Agrartechnik Bornim e. V.
Abteilung Technik in der Tierhaltung
Max-Eyth-Allee 100
14469 Potsdam
Tel.: +49/(0)331/5699-514
Fax: +49/(0)331/5699-849
E-mail: bmoeller@atb-potsdam.de